

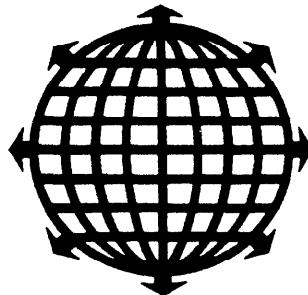
NATIONAL RENEWABLE ENERGY LABORATORY
LIBRARY

SEP 7 1995

GOLDEN, COLORADO 80401-3393

**PROCEEDINGS OF
SOLAR '95
THE 1995
AMERICAN SOLAR ENERGY SOCIETY
ANNUAL CONFERENCE**

**Minneapolis, Minnesota
July 15-20, 1995**



**Editors:
R. Campbell-Howe
B. Wilkins-Crowder**

**American Solar Energy Society
2400 Central Avenue, Suite G-1
Boulder, CO 80301**

Printed on recycled paper

COMPARISON OF NATURAL CONVECTION HEAT EXCHANGERS FOR SOLAR WATER HEATING

Scott D. Dahl
Jane H. Davidson
University of Minnesota
Department of Mechanical Engineering
111 Church Street S.E.
Minneapolis, MN 55455

ABSTRACT

The use of natural convection, side-arm heat exchangers in solar domestic water heating systems is becoming a popular method of reducing system cost and electric demand. In this paper, we compare thermal performances of three natural convection heat exchangers mounted along the outside of the water storage tank and a commercial wrap-around-tank heat exchanger to two forced-flow heat exchangers. The external natural convection heat exchangers are 1) a commercial, single-wall, coil-in-shell design, 2) a double-wall, two-pass, tube-in-shell exchanger and 3) a single-wall, single-pass, tube-in-shell design. Performance is discussed in terms of pressure drop, heat exchanger effectiveness, and overall heat transfer coefficient. Measured data were either obtained in our laboratory or from previously reported studies. Heat transfer area appears to be the most significant factor in determining thermal performance. Because its heat transfer area is three times larger, the commercial coil-in-shell heat exchanger has natural convection flow rates nearly three times greater than the two tube-in-shell designs.

1. INTRODUCTION

A recent innovation in solar domestic hot water systems is the use of natural convection heat exchangers (NCHX), as shown in Fig. 1. Like traditional anti-freeze systems, the heat exchanger is external to the storage tank, but flow in the tank loop is buoyancy-driven rather than pumped. The primary advantages of any NCHX are reduced capital and maintenance costs and lower electric demand since a pump is eliminated. A few electric utilities are now promoting the use of solar water heating systems to reduce demand for electricity or shift the demand to off-peak hours [1].

Other heat exchange options that compete with the external NCHX are in-tank heat exchangers and wrap-around heat exchangers. The main advantage of external NCHXs over these competing technologies is that they can be used with

conventional water heaters and are easily retrofit to existing tanks.

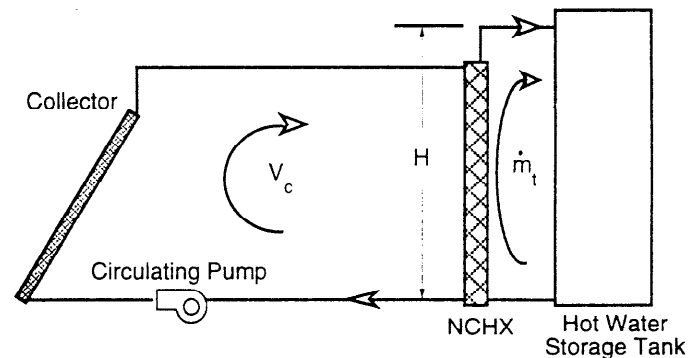


Fig. 1. General schematic of a solar water heating system with a natural convection heat exchanger.

The flow rate of water on the tank-side of a NCHX depends on density differences throughout the tank loop and hydraulic resistance across the heat exchanger as well as connecting piping. The density differences depend on the amount of heat transfer across the heat exchanger as well as the state-of-charge of the storage tank. Using a 1-D assumption, the natural convection flow rate can be determined from a pressure balance on the water loop:

$$\Delta P_{f,HX} + \Delta P_{f,pipe} = \int_0^H \rho(T) g dy \Big|_{\text{tank}} - \int_0^H \rho(T) g dy \Big|_{HX}, \quad (1)$$

where flow rate is contained in the expressions for pressure drop due to shear across the heat exchanger ($\Delta P_{f,HX}$) and frictional pressure drop in the connecting piping ($\Delta P_{f,pipe}$). In eqn. (1), the height, H , is measured from the bottom of the tank and includes any vertical pipes necessary to connect the heat exchanger to the top of the tank. The frictional loss in the tank is neglected. The hydrostatic

pressure difference on the right hand side of eqn. (1) can be considered the force driving the natural convection flow.

In this paper, performances of three natural convection heat exchangers are compared for collector flow rates of 0.02 L/s and 0.03 L/s. Schematics of the three heat exchangers are shown in Figs. 2 through 4. Buoyancy-driven flow is on the shell-side for all three designs. The two-pass and single-pass tube-in-shell designs, shown in Figs. 2 and 3 and tested in our laboratory, are not commercially available. Needle fins in the single-pass, single-wall heat exchanger are intended to enhance heat transfer on the natural convection-side of the exchanger. Heat transfer areas of both are estimated to be approximately 0.2 m². (Area of the single-pass, spiked heat exchanger is based on a guess of the surface area of the fins.) The multiple coil-in-shell heat exchanger is available commercially and was evaluated at the University of Waterloo [2-4]. Its heat transfer area is 0.61 m². Comparison of the performance of the heat exchangers is based on measured values of $\dot{A}P_{f,HX}$, heat exchanger effectiveness (ϵ), and the overall heat transfer coefficient-area product (UA) as functions of natural convection flow rate. Since a recently developed model for systems using NCHXs [2,5] requires measured values of modified heat exchanger effectiveness (ϵ'),

$$\epsilon' = \frac{T_{h,i} - T_{h,o}}{T_{h,i} - T_{c,i}}, \quad (2)$$

we also present a comparison of this quantity.

In addition, we compare UA values of the NCHXs to those of a wrap-around heat exchanger [6], and two conventional double-wall heat exchangers with forced flow on both sides [7,8]. The wrap-around heat exchanger is a commercial product which has a 36.6-m length of 1.59-cm diameter copper tubing wrapped around the outside of the lower-half of a water storage tank. We estimate the heat transfer area of the wrap-around exchanger to equal the inside wall surface area of the bottom-half of the tank, approximately 1 m².

One of the forced-flow heat exchangers is a counter-flow, double-walled, tube-in-tube design with a heat transfer area of 0.21 m². The inside tube is identical to the tube in the tube-in-shell NCHX shown in Fig. 2. The other forced-flow heat exchanger is an eight-pass, counter-flow, double-walled, smooth tube-in-tube design with a heat transfer area of 0.28 m².

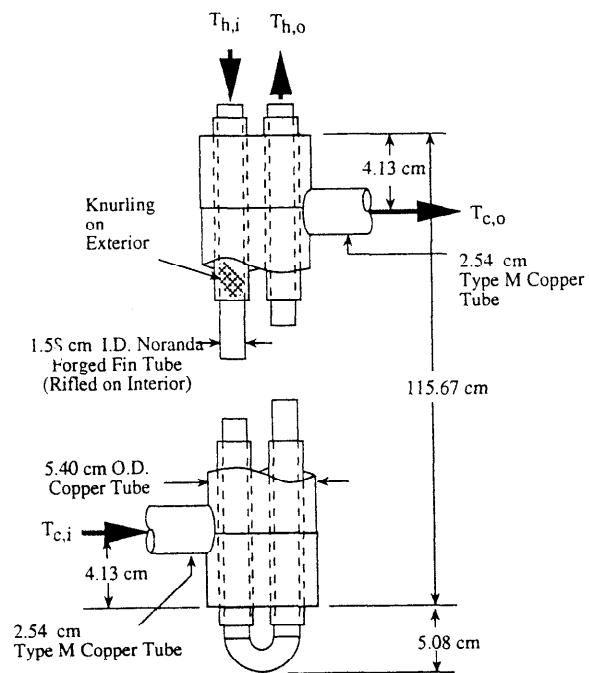


Fig. 2. Two-pass, double-wall, tube-in-shell heat exchanger.

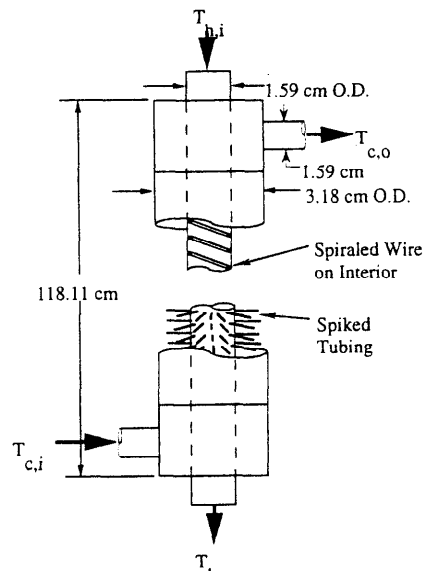


Fig. 3. Single-Pass, single-wall, with enhanced heat transfer surfaces, tube-in-shell heat exchanger.

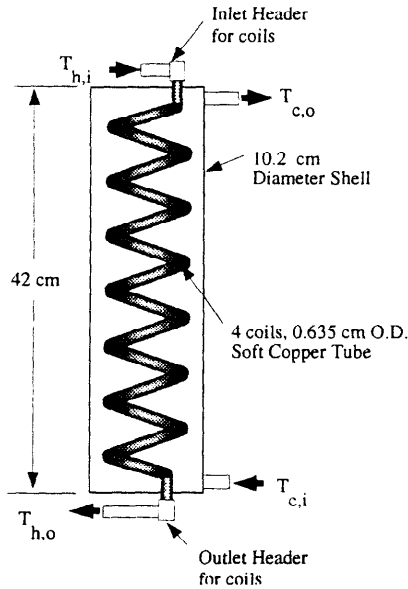


Fig. 4. Multiple coil-in-shell heat exchanger. Adapted from schematics in [2].

2. DESCRIPTION OF DATA SOURCES

Testing of the two NCHXs shown in Figs. 2 and 3 was conducted in our laboratory in a facility that consists of two water loops on either side of the heat exchanger: a simulated collector loop in which heat is input with an electric boiler, and a storage tank loop [9]. Frictional pressure drop across the heat exchanger positioned horizontally was measured with pumped flow and with no heat input. "Collector" flow rate and temperature differences across the heat exchangers were measured and then natural convection mass flow rate was determined from an energy balance. We began each test with an isothermal tank at 21°C. The collector loop temperatures were then stepped up in 5°C increments from the initial tank temperature to approximately 96°C. All the measurements were made at steady-state for each temperature setting. The water in the storage tank was allowed to stratify during the 6 hour tests.

Experimental data for the coil-in-shell heat exchanger measured at the University of Waterloo [2-4] were also acquired during steady-state tests of the heat exchanger with a simulated collector. The primary difference in their experimental procedure and ours is that during their tests, the tank was maintained at a constant temperature of 30°C for $V_c=0.02$ L/s and at 21°C for $V_c=0.03$ L/s. Water in the tank was kept at a constant temperature by adding cold water to the top and removing the same amount of water from the bottom of the tank. As in our experiments, natural convection flow rate was determined from an energy balance. The pressure drop due to shear across the heat exchanger was determined from measurements obtained with the exchanger operating in its normal orientation with pumped flow and no heating. Since neither UA nor ϵ was reported, these values were calculated using tabulated inlet temperature measurements and water outlet temperature measurements obtained from plots in [2]. Values of

modified effectiveness were determined from plots of ϵ' versus natural convection flow rate.

Measurements of UA for the forced-flow heat exchangers were obtained in an OG-200 test [10] with a simulated collector flow rate of 0.114 L/s and a water-side flow rate of approximately 0.170 kg/s [7,8].

Performance of the wrap-around heat exchanger was evaluated with a simulated collector-side flow rate of 0.03 L/s with a constant heat flux input of approximately 2000 W [6].

Heat exchanger performance is described by UA, ϵ , and ϵ' , which is given in eqn. (2). The value of UA was determined from,

$$UA = \frac{(\dot{m}c_p)_t(T_{c,o} - T_{c,i})}{\text{LMTD}}, \quad (3)$$

where the log-mean-temperature-difference (LMTD) for the external NCHXs and forced-flow heat exchangers is given by,

$$\text{LMTD} = \frac{(T_{h,o} - T_{c,i}) - (T_{h,i} - T_{c,o})}{\ln[(T_{h,o} - T_{c,i})/(T_{h,i} - T_{c,o})]}. \quad (4)$$

LMTD for the wrap-around heat exchanger is defined by [6] as,

$$\text{LMTD} = \frac{(T_{h,i} - T_{\text{tank,HX top}}) - (T_{h,o} - T_{\text{tank,HX bottom}})}{\ln[(T_{h,i} - T_{\text{tank,HX top}})/(T_{h,o} - T_{\text{tank,HX bottom}})]}, \quad (5)$$

where $T_{\text{tank,HX top}}$ and $T_{\text{tank,HX bottom}}$ correspond to the temperatures in the tank near the top and bottom of the wrap-around heat exchanger, respectively.

Heat exchanger effectiveness is determined as,

$$\epsilon = \frac{(\dot{m}c_p)_h(T_{h,i} - T_{h,o})}{(\dot{m}c_p)_{\min}(T_{h,i} - T_{c,i})}. \quad (6)$$

3. RESULTS

Characteristics of the single-pass, two-pass, and coil-in-shell NCHXs are compared in Figs. 6 through 10. The error bars reported in the plots represent the uncertainty in the measurements for the two tube-in-shell heat exchangers tested in our laboratory.

In Fig. 6, pressure drops across the natural convection (shell) side of the NCHXs are plotted as a function of natural convection flow rate. Pressure drop across the pipes connecting the heat exchangers to the tank are not included in this measurement. The two-pass tube-in-shell and the coil-in-shell heat exchangers have very similar pressure drop characteristics. The higher pressure drop across the

single-pass design is attributed to the presence of the spiked fins. For a given heat transfer surface area and flow rate, it is obvious from eqn. (1) that a lower pressure drop is desired for maximum flow rate. Optimal water flow rate is a function of collector characteristics as well as the design of the tank. Lowering flow rates to achieve thermal stratification may decrease the energy transferred in the heat exchanger and thus reduce system performance. An alternative approach is to maximize flow rate and use some type of manifold to maintain stratification in the tank [11].

Figs. 7 and 8 are plots of heat exchanger effectiveness and UA, respectively, as functions of the natural convection and collector forced-flow rates for the three NCHXs. The most important feature of the data in these plots is the difference in natural convection flow rates achieved in the coil-in-shell heat exchanger as compared to those achieved in the tube-in-shell designs. The maximum flow rate attainable in the tube-in-shell heat exchangers was 0.012 kg/s whereas buoyancy-induced flow rate in the commercial coil-in-shell was as high as 0.035 kg/s (still substantially less than typical pumped-flow rates in most indirect systems). Since the coil-in-shell heat exchanger has a heat transfer area nearly three times larger than the two other NCHXs, more energy is transferred to the cold fluid with the same inlet conditions and the driving force for natural convection flow (the hydrostatic pressure difference on the right hand side of eqn. (1)) is much greater. In addition, since the coil-in-shell heat exchanger is shorter, water densities over much of the height H are lower than in the other heat exchangers. This difference also increases the driving force by reducing the hydrostatic pressure in the heat exchanger section of the loop. Since we do not know the pressure loss across the pipes connecting the coil-in-shell heat exchanger to the tank, we cannot speculate on the effect of this loss on flow rate in the present analysis. The effect of the pressure loss in the connecting piping could substantially affect the natural convection flow rate.

In Fig. 8, the value of UA is controlled by the natural convection flow rate. The heat transfer coefficient on the force-flow side of the tubes is much larger than the heat transfer coefficient on the natural convection side.

The maximum energy transferred (at the maximum natural convection flow rate) in the two tube-in-shell NCHXs was approximately 2500 W, compared to nearly 5500 W for the coil-in-shell design.

In Fig. 9, the overall heat transfer coefficient, U , determined by dividing UA by the estimated heat transfer area of each heat exchanger, is plotted. For the range of natural convection flow rates over which all the heat exchangers operate (up to ≈ 0.012 kg/s), there is no significant difference in values of heat transfer coefficient. Heat transfer area appears to be the limiting factor to improved performance.

To put the performance of the NCHXs in perspective, values of UA and U for the external NCHXs, and the wrap-around heat exchanger are compared to those of two forced-flow heat exchangers (operating with flow rates typical of a water heating system with two collectors) in Table 1.

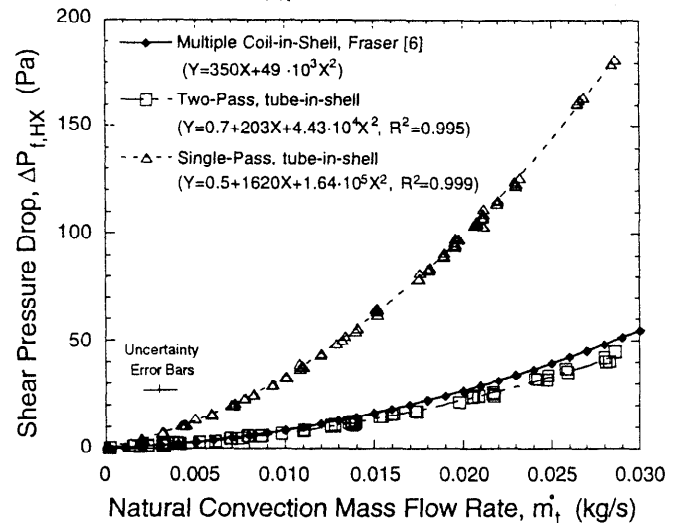


Fig. 6. Shear Pressure drop ($\Delta P_{t,HX}$) plotted as a function of natural convection mass flow rate (\dot{m}_t).

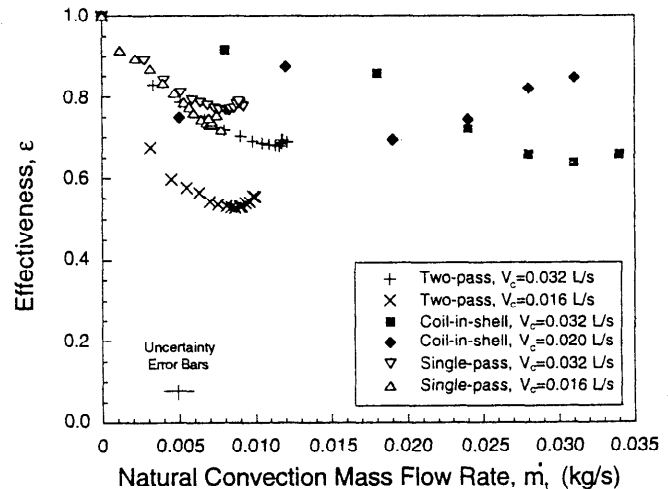


Fig. 7. Effectiveness (ϵ) plotted as a function of natural convection mass flow rate (\dot{m}_t) and volumetric flow rate (V_c) on the collector side of the heat exchanger.

Higher flow rates in the pumped heat exchangers result in much higher heat transfer coefficients. With the natural convection heat exchangers, U values are similar at the same flow rate. The coil-in-shell and wrap-around heat exchangers have higher UA values than the other NCHXs because of their larger heat transfer surfaces. Increasing collector-side flow rate in the wrap-around heat exchanger does not increase UA since, like the other NCHXs, UA is restricted by the water-side heat transfer coefficient.

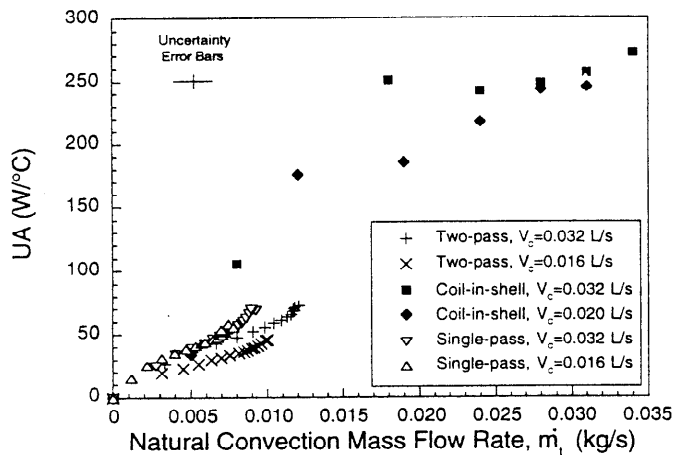


Fig. 8. Overall heat transfer coefficient-area product (UA) plotted as a function of natural convection mass flow rate (\dot{m}_l) and volumetric flow rate (V_c) on the collector side of the heat exchanger.

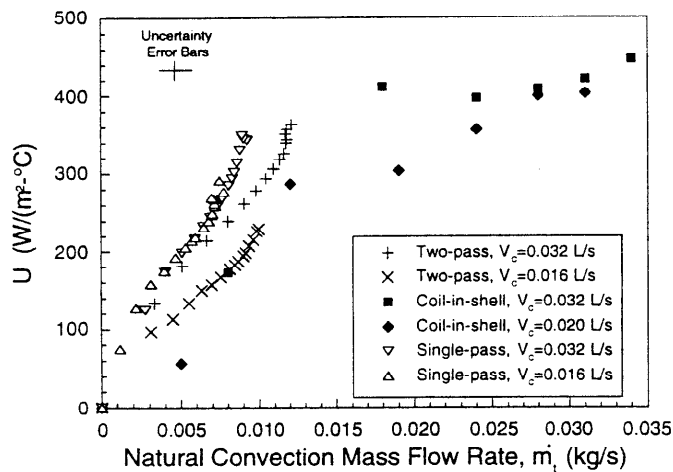


Fig. 9. Overall heat transfer coefficient (U) plotted as a function of natural convection mass flow rate (\dot{m}_l) and the volumetric flow rate (V_c) on the collector side of the heat exchanger.

Since modified effectiveness is not traditionally used to characterize heat exchangers, we only present it in Fig. 10 for readers interested in using the recently developed model [5]. In general, a high value of modified effectiveness is desired since as ϵ' approaches 1, the maximum temperature drop across the collector (hot) side of the heat exchanger is obtained.

4. CONCLUSION

Comparison of three external NCHX designs indicates that increasing the heat transfer area without significantly increasing the pressure drop on the natural convection flow loop increases natural convection flow rates and thus the energy transfer to the tank. Friction losses in the connecting

TABLE 1. COMPARISON OF UA

HX	V_c L/s	\dot{m}_l kg/s	UA W/°C	U W/(m²·°C)
Forced-flow, eight-pass [7,8]	0.114	0.17	120	430
Forced-flow, single-pass [7,8]	0.114	0.17	175	818
Wrap-around [6]	0.032	-	188	188
NCHX coil-in-shell [2]	0.03	0.01	150	246
NCHX single-pass	0.032	0.01	70	350
NCHX two-pass	0.032	0.01	50	250

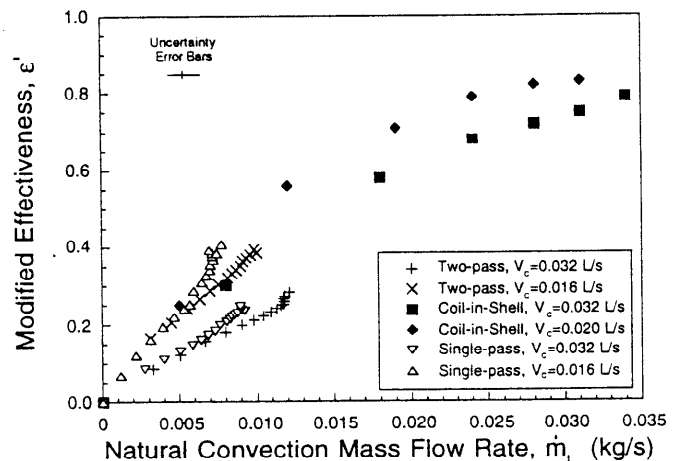


Fig. 10. Modified effectiveness (ϵ') plotted as a function of natural convection mass flow rate (\dot{m}_l) and volumetric flow rate (V_c) on the collector side of the heat exchanger.

pipng should be minimized to decrease the resistance to flow.

The commercial coil-in-shell heat exchanger has natural convection flow rates nearly three times greater than the two tube-in-shell designs because the heat transfer area is three times larger. The U-values for all designs are nearly identical. The wrap-around heat exchanger, with the largest heat transfer surface area, has a UA similar to the coil-in-shell. The disadvantage is that a non-conventional tank is required and thermal stratification of the tank is not possible. The forced flow heat exchangers have higher U-values, due to greater water flow rates, but at a cost of increased electrical energy to operate the water-loop pump.

5. NOMENCLATURE

c_p	=	specific heat
g	=	acceleration of gravity, m/s^2
H	=	height of the heat exchanger/tank loop, m
\dot{m}_n	=	natural convection mass flow rate, kg/s
P	=	pressure, Pa
R^2	=	coefficient of determination
T	=	temperature, $^{\circ}C$
U	=	overall heat transfer coefficient, $W/(m^2 \cdot ^{\circ}C)$
UA	=	overall heat transfer coefficient-area product, $W/^{\circ}C$
V	=	volumetric flow rate, L/s
y	=	vertical coordinate, m
<u>Greek Letters</u>		
Δ	=	difference
ε_e	=	heat exchanger effectiveness, eqn. (6)
ε	=	modified heat exchanger effectiveness, eqn. (2)
ρ	=	fluid density, kg/m^3
<u>Subscripts</u>		
c	=	cold
C	=	collector
f	=	frictional
h	=	hot
i	=	inlet
HX	=	heat exchanger
min	=	minimum
o	=	outlet
$tank$	=	refers to the water storage tank
$pipe$	=	connecting piping between the tank and HX
t	=	natural convection/tank side of heat exchanger

6. ACKNOWLEDGMENTS

The support of this work by Mr. Robert Hassett of the United States Department of Energy and the University of Minnesota is appreciated.

7. REFERENCES

- [1] C.S. and Osborn, D.E., 1994, "SMUD's Residential and Commercial Solar Domestic Hot Water Programs." *Solar '94, Proceedings of 1994 Annual Conference of the American Solar Energy Society*, pp. 267-272
- [2] Fraser, K.F., 1992, "Modelling Natural Convection Heat Exchangers in Solar Domestic Hot Water Systems," M.A.Sc. Thesis, Department of Mechanical Engineering, University of Waterloo, Waterloo, Canada
- [3] Fraser, K.F., Hollands, K.G.T., and Brunger A.P., 1992, "Modelling Natural Convection Heat Exchangers for SDHW Systems," *Proceedings of the 18th Annual Conference of the Solar Energy Society of Canada*, pp. 190-195
- [4] Fraser, K.F., Hollands, K.G.T., and Brunger A.P., 1993, "Validation of a Model for Natural Convection Heat Exchangers in SDHW Systems," *Proceedings of the ISES Solar World Congress*, pp. 219-224
- [5] Avina, J., 1994, "The Modeling of a Natural Convection Heat Exchangers in a Solar Domestic Hot Water System," M.S. Thesis, Department of Mechanical Engineering, University of Wisconsin, Madison
- [6] Miller, J.A. and Hittle, D.C., 1995, "Experimental Evaluation of a Simulation Model for Wrap-Around Heat Exchangers, Solar Storage Tanks," *Proceedings of the ASME/JSME/JSES International Solar Energy Conference*, pp. 1117-1124, Maui, Hawaii
- [7] Thornbloom, M.D., 1992, "Impact of Flow Rates and Heat Exchanger Design on Indirect Solar Water Heating System Performance," M.S. Thesis, Department of Mechanical Engineering, Colorado State University, Fort Collins
- [8] Thornbloom, M.D. and Davidson, J.H., 1992, "Influence of Heat Exchanger Effectiveness and System Flow Rates on Experimental Rating of a Generic Antifreeze SDHW System," *Solar '92*, pp. 123-128. Presented at the ASES Solar Energy Conference, Cocoa Beach, June
- [9] Dahl, S.D. and Davidson, J.H., 1995, "Characterization of a Tube-in-Shell Thermosyphon Heat Exchanger for Solar Water Heating," *Proceedings of the ASME/JSME/JSES International Solar Energy Conference*, pp. 1157-1163, Maui, Hawaii
- [10] Solar Rating and Certification Corporation, Washington, D.C., 1984, *Test Methods and Minimum Standards for Certifying Solar Water Heating Systems*, Standard 200-82
- [11] Adams, D. and Davidson, J.H., 1994, "Fabric Stratification Manifolds for Solar Water Heating," *Journal of Solar Energy Engineering*, Vol. 116, pp. 130-136